Ultrasonics 119 (2022) 106588

Contents lists available at ScienceDirect

Ultrasonics

journal homepage: www.elsevier.com/locate/ultras

Magnetic domain wall motion driven by an acoustic wave

Evgeny Vilkov [a,*], Oleg Byshevski-Konopko [a], Pavel Stremoukhov [b,c], Ansar Safin [d,e], Mikhail Logunov [d], Dmitry Kalyabin [c,d], Sergey Nikitov [c,d], Andrei Kirilyuk [b,d]

[a] Kotelnikov Institute of Radio Engineering and Electronics, Fryazino Branch, Russian Academy of Sciences, Moscow oblast, Fryazino, 141190, Russia
[b] FELIX Laboratory, Radboud University, Toernooiveld 7, 6525 ED Nijmegen, The Netherlands
[c] Moscow Institute of Physics and Technology, Dolgoprudny, Moscow Region, 141700, Russia
[d] Kotel'nikov Institute of Radioengineering and Electronics, Russian Academy of Sciences, 125009, Moscow, Russia
[e] National Research University "Moscow Power Engineering Institute", 111250, Moscow, Russia

ARTICLE INFO

Keywords:
Domain wall
Acoustic waves
Spin waves

ABSTRACT

Dynamic interaction of acoustic and magnetic systems is of strong current interest, triggered by the promises of almost lossless new concepts of magnet-based information technology. In such concepts, a significant role is often given to domain walls (DW). Therefore, here we investigate how launching an acoustic shear wave, we can control the DW motion. Surprisingly, at sufficiently large amplitudes of the shear displacement, the speed of the forced DW motion can reach sizeable fraction of the speed of sound. This was shown to happen due to certain resonance conditions depending on the wave frequency, its angle of incidence, and shear displacement amplitudes, leading to a total reflection of the wave and maximizing the impact. Most interesting, strong nonlinearity appears in the interaction of the elastic and magnetic subsystems, expressed by the negative slope of the resonant reflection peak and the s-shaped dependence of the domain wall velocity on the shear displacement amplitude, typical for nonlinear systems.

1. Introduction

Waves are everywhere: human beings see, interact and communicate through light and sound waves. Light is instrumental to transport massive amounts of data. Radiowaves and microwaves enable long distance communication and GPS systems. The research on waves is increasingly directed to the possibilities to gain full control over these waves and use them to manipulate matter. The ultimate question is: what are the limits to changing material properties with waves that are tailored in space and time? And then: what are the new concepts that can arise from these limits?

The most popular type of the waves used to study and manipulate matter is of cause the electromagnetic radiation. In magnetic materials in particular, short laser pulses were shown to be able to rapidly change magnetization on a sub-picosecond time scale [1]; to modify magnetic anisotropy [2]; to trigger magnetic precession and spin waves [3,4]; and even to reverse the magnetization [5–7]. However, the applications of ultrafast optical methods are often limited by the simultaneous generation of a significant number of non-equilibrium charge carriers and as a consequence, a considerable increase in material temperature. Because of this, other wave-driven processes are being considered. Among them, the interaction of acoustic waves with magnetic systems becomes increasingly popular because of lower dissipation and much better scaling-down prospects.

In particular, the so-called *straintronics* is a novel research direction in magnetism with promising applications [8], that represent an outstanding alternative to other wave-based approaches because of the very low damping of acoustic waves (phonons) as compared to magnons or plasmons [9,10]. Magnetic straintronics was indicated to be able to realize memory units with the switching energy of below 1 aJ, which is already very close to the theoretical Landauer limit of $k_B T \ln 2$ [11,12]. Therefore, specifics of the interaction between magnon and phonon subsystems have recently become an area of strong interest [13–16], from acoustically driven ferromagnetic resonance [17], to magneto-elastic manipulation of magnetic bubbles [18], and to a complete ultrafast phonon-driven magnetic switching [19].

In general, fast and efficient control of magnetization is central in information storage and processing technologies based on magnetic materials, where magnetic domains serve as bits of information. In contrast, magnetic *domain walls* (DW) represent an interesting alternative as a basis for various spintronic devices [20,21]. Being a flexible magnetic phase boundary, DWs can be used as elements of integrated spintronics such as logic gates, memory bits and so on. However, what

* Corresponding author.
E-mail address: e-vilkov@yandex.ru (E. Vilkov).

https://doi.org/10.1016/j.ultras.2021.106588
Received 20 July 2021; Received in revised form 4 September 2021; Accepted 15 September 2021
Available online 24 September 2021

severely hampers the application of DW-related concepts in technology, is that the magnetic field, typically required to control them, is a very inefficient, bulky, and energy-consuming factor. This is the reason why other stimuli to control the DW motion are being widely investigated at present.

In this paper, we theoretically investigate the possibility to drive magnetic domain wall motion employing a bulk shear wave. Shear waves are of importance in many applications, such as structural health monitoring and nondestructive testing [10], manipulation of small objects [22,23], or in microelectromechanical systems (MEMS) [24]. Via magnetostriction effect, shear waves can be effectively induced in magnetic media [25], while the inverse effects allow the acoustic waves to influence the magnetization, also depending on the applied magnetic field [26].

Originally, the problem of interaction of DW with acoustic waves in ferromagnetic crystals was in some way inspired by the studies of similar effects of parametric interaction of electromagnetic radiation with moving interfaces — mirrors in optics and electrodynamics [27]. In particular, electromagnetic waves reflected from moving magnetic "mirrors" in ferrites [28] could be used to measure the velocity of fast moving DW [29] and to study its interaction with phonons [30].

In this work we show how an acoustic wave induces the DW motion when incident at an angle onto the plane of the wall (Fig. 1(a)). First of all, a propagating shear wave creates, via magneto-elastic interaction, small oscillating effective magnetic fields. Crossing DW, however, results in an extra contribution to magnetic potential and creates a periodic pattern of magnetostatic leakage field poles of alternating sign (see Fig. 1(b)). Because of these poles that couple back into the elastic system, a reflected wave appears. This reflection, that only occurs at a finite angle of incidence (otherwise, no poles are created!), creates a certain pressure on DW, depending on the reflection coefficient. This pressure, that can in principle lead to the motion of DW, is typically a small effect only. However, when the frequency of the acoustic wave approaches that of ferromagnetic resonance, these oscillating poles lead to a large-amplitude precession of spins in the vicinity of DW and, surprisingly, to a total reflection of the wave. The resulting pressure becomes significant, creating an effective mechanism to drive the DW dynamics.

Most interesting, the resonant coupling of the magnetic and acoustic subsystems, together with nonlinear properties of magnetoelastic interaction, can lead to various unusual effects [32]. For example it has been shown that such nonlinear effects are important for spin wave propagation, and that they can directly be observed experimentally [32,33]. In our case, the nonlinearity is strongly expressed by the negative slope of the resonant reflection peak and the s-shaped dependence of the domain wall velocity on the amplitude of shear displacement.

The paper is organized as follows: general formulation of the problem, magnetic energies and the equation of motion are given in Section 2. Section 3 discusses in general the evaluation of the pressure on the wall resulting from the reflection of the incident acoustic wave from it. Further, Section 4 deals with the wave refraction on DW and the resulting from it magnetic poles, in the static case. Section 5 adds the DW motion and derives the final equations for the reflection and transmission coefficients in this case. Finally, Section 6 shows the results of numerical simulations and treats the appearing nonlinearities. The paper closes with conclusive discussions in Section 7.

2. Formulation of the problem

The geometry of our model is shown in Fig. 1(a). Acoustic waves are excited on the (010)-oriented face of YIG crystal, and propagate in the xy-plane orthogonal with respect to the magnetization of the domains as well as to the internal magnetic field, that are both directed along the z-axis: $\mathbf{M}_0$, $\mathbf{H}_i \parallel \mathbf{z}$, thus the wave vector $\mathbf{k} \perp \mathbf{H}_i, \mathbf{M}_0$. The excitation source by itself is not important here; they can be excited using various mechanisms, such as optical [34,35], piezoelectric [36], acoustic [37],

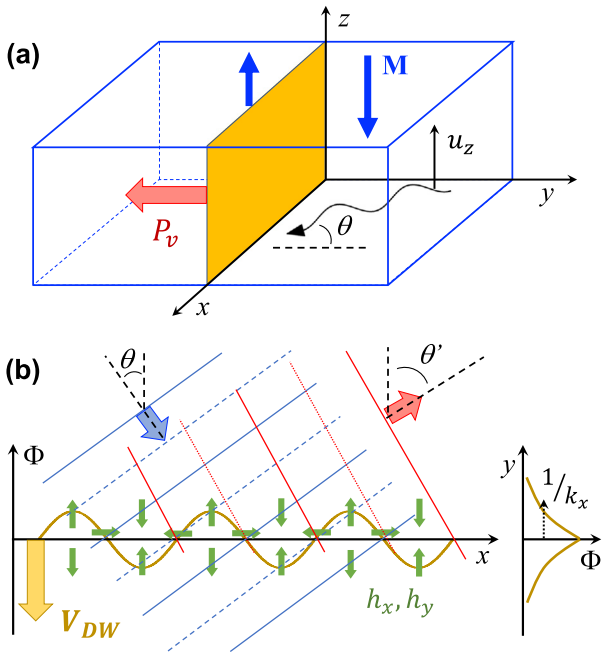

Fig. 1. (a) The geometry considered in this work: DW is placed in the xz plane of YIG crystal. The acoustic wave is incident on the DW under an angle θ in the xy-plane. The magnetization in the two domains is along the $\pm z$-axis, as well as the polarization u_z of the incident shear wave. P_v is the pressure on DW created by the incident wave. (b) A toy model showing the sinusoidal distribution of the DW-induced magnetic potential Φ (yellow line) as well as the local oscillating magnetic fields h_x, h_y resulting from it (green arrows). Note that the incident (θ) and reflection (θ') angles are not equal, which is the result of the Doppler effect [31]. k_x is the x-component of the wave vector of the incident wave.

and others [35,36]. Acoustic waves are treated in a harmonic plane wave approximation as purely shear waves with particle displacements $\mathbf{u} \parallel \mathbf{z}$. In this case $u_{ii} = \mathrm{div} u \equiv 0$ and deformation tensor u_{ik} has the following non-zero components:

$$u_{xz} = u_{zx} = \frac{1}{2}\frac{\partial u_z}{\partial x}, \quad u_{yz} = u_{zy} = \frac{1}{2}\frac{\partial u_z}{\partial y} \tag{1}$$

The energy density of the crystal is given by

$$w = w_M + w_H + w_{MU} + w_U\,, \tag{2}$$

where w_M is the magnetic energy density, w_H is the sum of Zeeman energy and magnetic dipole–dipole interaction energy, w_{MU} is the density of magnetoelastic interaction, w_U is the elastic energy density. The magnetic density w_M has the following form

$$w_M = w_a + w_e \tag{3}$$

namely, it is the sum of the magnetic anisotropy w_a and the exchange interaction:

$$w_e = \frac{1}{2}\alpha_{ik}\frac{\partial \mathbf{M}}{\partial x_i}\cdot\frac{\partial \mathbf{M}}{\partial x_k}\,. \tag{4}$$

Here α_{ik} is the tensor of the exchange interaction coefficients, diagonal in cubic ferrites: $\alpha_{ik} = \alpha\delta_{ik}$.

The vectors $\mathbf{M}$ and $\mathbf{H}$ are represented as the sum of the static (equilibrium) part and the small dynamic term that appear due to the acoustic wave as

$$\mathbf{H}(t) = \mathbf{H}_i + \mathbf{h}(t), \quad \mathbf{M}(t) = \mathbf{M}_0 + \mathbf{m}(t)\,, \tag{5}$$

where $\mathbf{H}_i$ is the vector of internal static magnetic field of the crystal, $\mathbf{M}_0$ is the vector of static magnetization and $\mathbf{h} \ll \mathbf{H}_i$, $\mathbf{m} \ll \mathbf{M}_0$. Neglecting higher order we obtain $w_a \approx K_1(m/M_0)^2$ for the anisotropy energy. We consider the crystal with a positive magnetic anisotropy constant $K_1 > 0$, which means that the easy anisotropy axes are along the main

axes of the cubic unit cell. Due to the assumed dependence of M on $r = (x, y, z)$, through a dynamic term to a field of the form $M \sim e^{i(kr)}$, expression (5) gives the following estimate $w_e \sim \alpha M^2 k^2$, where k is the wave number. Hence, according to the following definition of the effective magnetic field: $\mathbf{H}_{\text{eff}} = -\partial w/\partial \mathbf{M}$ [38,39], we obtain the expressions for estimating the contributions of the magnetic anisotropy and exchange interaction in the field $\mathbf{H}_i$ of the crystal as

$$H_a \sim 2K_1 \frac{|M|}{M_0^2} \approx 2\frac{K_1}{M_0}, \quad H_e \sim \alpha M k^2 \tag{6}$$

It follows from Eq. (6) that the static contribution of H_a only leads to renormalization of the external magnetic field H_0 to the value $\mathbf{H}_i = \mathbf{H}_0 + \mathbf{H}_a$, called the internal magnetic field. Thus, when deriving the initial equations of magnetoacoustics, there is no need to include the magnetic anisotropy at intermediate stages. It is more convenient to do this at the end by resorting to the above renormalization of the static field.

In addition, comparing the exchange interaction in garnets [38,40] with the values of the internal magnetic fields $\mathbf{H}_i$ for the regions of homogeneous magnetization (domains), it is always possible to select such a spectral region where $H_e \ll H_i$. For YIG, for example, we have $H_i < 10^3$ Oe, and exchange stiffness $D = \alpha M_0 \sim 5 \cdot 10^{-9}$ Oe cm^2. Therefore, according to Eq. (6), we have $Dk^2 \ll H_i$ if $k < 10^5$ cm^{-1}. So, assuming in what follows that we are in just such a part of the spectral region where the exchange interaction can be neglected, we will take in Eq. (3) $w_e = 0$. Also taking into account the anisotropy by renormalizing H_i, this allows us to take $w_M = 0$ in Eq. (2). In this approximation, a domain wall can be considered as a structureless and extremely thin boundary, which considerably simplifies the treatment of this problem.

Next, for w_H we have [39]:

$$w_H = -\mathbf{M} \cdot \mathbf{H} + \frac{1}{8\pi}\mathbf{H}^2 .$$

Here, the second term is the energy density of the magnetic dipole interaction caused by the demagnetizing fields that appear due to the limited size of the crystal. In what follows, we assume that the crystal is infinite (in practice, this corresponds to the sample size $L \gg 2\pi/k$) and do not take this second term into account. As for the first term, it represents the usual Zeeman energy.

So, taking into account $w_M = 0$, $w_H \approx -\mathbf{M} \cdot \mathbf{H}$, and including the magnetostatic approximation and renormalization of H_i, the required energy densities are given by

$$w_H = -\mathbf{M}_0 \cdot \mathbf{H}_i \tag{7}$$

$$\begin{aligned} w_{MU} &= 4b_{44} M_0 (m_x u_{zx} + m_y u_{zy}) \\ &= (2\beta/M_0)(m_x u_{zx} + m_y u_{zy}) \end{aligned} \tag{8}$$

$$w_U = 2\lambda_{44}(u_{zx}^2 + u_{zy}^2) = \frac{\lambda_{44}}{2}(\nabla u_z)^2 = \frac{\lambda_{44}}{2} k^2 u_z^2 , \tag{9}$$

where $\beta = 2b_{44} M_0^2$ is the constant of magnetoelastic interaction, λ_{44} is the element of the shear modulus tensor, $u_{xz} = u_{zx} = \frac{1}{2}\frac{\partial u_z}{\partial x}$, $u_{yz} = u_{zy} = \frac{1}{2}\frac{\partial u_z}{\partial y}$.

Let the small dynamic terms $\mathbf{h}$, $\mathbf{m}$ depend only on the coordinates in the incidence plane of the wave, i.e. xy-plane. Taking into account the smallness of these terms and the orientation of the static fields along the z-axis, we take $M_{x,y} = m_{x,y}$, $M_z \approx M_0$, $H_{x,y} = h_{x,y}$, $H_z \approx H_i$. The static fields $\mathbf{H}_i$, $\mathbf{M}_0$ can be considered homogeneous: $H_i, M_0 = const$, due to the fact that the demagnetizing fields are not taken into account. Such linear approximation imposes restriction on the amplitude of shear waves as $u_z < 10^{-9}$ cm, which follows from numerical estimates.

To describe our problem, we combine the equation of motion from elasticity theory with the Landau–Lifshitz equations for magnetic moments [41,42]:

$$\rho \frac{\partial^2 u_z}{\partial t^2} = \lambda_{44} \nabla^2 u_z + \frac{\beta}{M_0}\left(\frac{\partial m_x}{\partial x} + \frac{\partial m_y}{\partial y}\right) \tag{10}$$

$$\begin{aligned} \frac{\partial m_x}{\partial t} &= -\gamma\left[m_y H_i + \beta\frac{\partial u_z}{\partial y} - M_0 h_y\right], \\ \frac{\partial m_y}{\partial t} &= -\gamma\left[m_x H_i + \beta\frac{\partial u_z}{\partial x} - M_0 h_x\right], \end{aligned} \tag{11}$$

where ρ is the density of the YIG crystal.

Eqs. (10), (11) must be supplemented by Maxwell's equations, that, due to the small value of the speed of acoustic waves as compared with the speed of light, can be treated in the quasi-static approximation [39]:

$$\nabla \cdot \mathbf{b} = 0, \quad \nabla \times \mathbf{h} = 0, \quad \mathbf{b} = 4\pi\mathbf{m} + \mathbf{h} , \tag{12}$$

where $\mathbf{b}$ is the induction of the dynamic magnetic field. Introducing the magnetostatic potential φ such that

$$\mathbf{h} = -\nabla\varphi , \tag{13}$$

and using Eq. (12) we obtain

$$\nabla^2\varphi = 4\pi\nabla \cdot \mathbf{m} . \tag{14}$$

Eqs. (10)–(14) represent the starting point of our treatment of shear waves in a ferromagnetic crystal.

3. Pressure by acoustic wave on domain wall

The pressure exerted by the shear wave on the DW, incident on the domain wall at an angle θ with respect to the normal to the DW plane, can be written as [37]:

$$\mathbf{P_0} = w_0[(1-T)\mathbf{i} + R\mathbf{i}']\cos\theta \tag{15}$$

where $w_0 = w_U + w_{MU}$ is the density of the energy carried by the wave (see Eqs. (8), (9)), T, R are the transmission and reflection coefficients, respectively, $\mathbf{i}$ is the unit vector in the direction of the incident wave on the DW and $\mathbf{i}'$ is the unit vector in the direction of the reflected wave from the DW. Taking into account that $R + T = 1$, Eq. (15) can be written in the form

$$P_0 = 2w_0 R\cos^2\theta . \tag{16}$$

For the numerical calculation of Eqs. (15)–(16), it is necessary to express the components of the dynamic magnetization in terms of the known variables. They can be easily found from Eqs. (11) as follows:

$$m_y = \frac{\gamma\beta}{\omega^2 - \omega_k^2}[-\omega k_x - ik_y\omega_0]\left\{1 + \frac{\omega_m\omega_0}{(\omega^2 - \omega_0^2)}\right\}u_z , \tag{17}$$

$$m_x = \frac{\gamma\beta}{\omega^2 - \omega_k^2}[-\omega k_y - ik_x\omega_0]\left\{1 - \frac{\omega_m\omega_0}{(\omega^2 - \omega_0^2)}\right\}u_z . \tag{18}$$

Let us now calculate the speed of the DW motion under the action of a sound wave. For generality, we also add an external magnetic field H_0 that creates and extra pressure on the DW as $P_H = 2M_0H_0$ [43]. In the case when the DW is not at rest, the pressure on it from the wave depends on the relative velocity of the wave and DW and is equal to $P_v = P_0(1 - V_{DW}/v_{gr})$, where V_{DW} is the DW velocity, $v_{gr} > 0$ the group velocity of the acoustic wave. The dissipative function of DW moving with velocity V_{DW} has the form

$$\Phi_d = -\frac{2\lambda}{\gamma^2}\sqrt{\frac{K_1}{\alpha}}V_{DW}^2 ,$$

where λ is the damping parameter [42]. Using Φ_d, we obtain the braking force of the DW per unit area as

$$P_\lambda = -\mu V_{DW}, \quad \text{where} \quad \mu = -\frac{2\lambda}{\gamma^2}\sqrt{\frac{K_1}{\alpha}}$$

From the condition of the steady-state motion $P_v + P_H + P_\lambda = 0$, we obtain the DW velocity as

$$V_{DW} = v_{gr}\frac{1 - 2M_0H_0/P_0}{1 + \mu v_{gr}/P_0} . \tag{19}$$

The formula for the steady-state velocity, obtained by taking into account the displacement by the applied field only, follows from Eq. (19) at $P_0 \to 0$ and has exactly the same form as in [42]:

$$V_H = \frac{\gamma^2 M_0 H_0}{\lambda}\sqrt{\frac{\alpha}{K_1}}$$

Thus, to obtain the DW velocity in the presence of acoustic waves, it is necessary to calculate the reflection coefficient of the waves from the domain wall, which in turn depends on the DW velocity.

4. Reflection of the wave from domain wall

Having determined the DW velocity in general, we will now consider the reflection of the wave from a static DW (interaction at the initial moment of time) as well as from the moving one. The Bloch wall is a transition region with a thickness $\Delta \approx \sqrt{\alpha/K_1}$ [38]. In the adopted exchangeless approximation, the value of α can be taken arbitrarily small. This serves as the basis for adopting a structureless geometric model of an infinitely thin Bloch wall corresponding to the limit $\alpha \to 0$, $\Delta \to 0$.

Taking into account the exchange interaction and, accordingly, the finite thickness of the domain wall and its structure [44], significantly complicates the problem even in the simplest case of normal incidence. However, only in the case of a very broad DW or for very high-frequency sound, the efficiency of the interaction between the acoustic wave and DW is expected to noticeably decrease.

The geometry of the problem is shown in Fig. 1. A geometrically thin structureless Bloch wall has the instantaneous coordinate y_{DW} and the velocity V_{DW}. Considering the spontaneous magnetizations $\mathbf{M}_0^{(j)}$ and internal magnetic fields $\mathbf{H}_i^{(j)}$ in the domains, we define them as

$$\begin{aligned} &M_0^{(j)} = (-1)^{j+1} M_0, \quad H_i^j = (-1)^{j+1} H_i, \\ &M_0 > 0, \quad H_i > 0\,, \end{aligned} \tag{20}$$

where $j = 1$ for $y > y_{DW}$, $j = 2$ for $y < y_{DW}$.

In addition to the condition $k\Delta \ll 1$, we also assume a weak dependence of the DW internal structure on the external stimuli, provided the system is far from phase transitions [45]. To exclude the magnetostrictive (Cherenkov) instability of the DW, we will assume that $|V_{DW}| < c_t$, where c_t is the shear wave velocity.

Elastic displacements $\mathbf{u}_z^{(j)}$ ($j = 1$ for $y > 0$, $j = 2$ for $y < 0$) and the potentials φ_j of the fields in the corresponding domains will satisfy Eqs. (10), (11), where, taking into account Eq. (20), the replacement $M_0 \to (-1)^{j+1} M_0$, $\omega_0 \to (-1)^{j+1}\omega_0$, $\omega_m \to (-1)^{j+1}\omega_m$ is carried out. Moreover, $\omega_0 = \gamma H_i$, and $\omega_m = 4\pi\gamma M_0$. We also replace u_z by $u_z^{(j)}$ in (2) and assume $h_j = -\nabla\varphi_j$. From Eqs. (10) and (11) we obtain for harmonic waves

$$\begin{aligned} &\nabla^2 u_j + (\rho\Omega^2/\lambda_\Omega^*)u_j = 0\,, \\ &\nabla^2\varphi_j = (-1)^{j+1}\frac{4\pi\gamma\beta\omega_0}{\Omega^2 - \omega_k^2}\nabla^2 u_j\,, \end{aligned} \tag{21}$$

where Ω is the frequency of the incident or refracted wave, $\lambda_\Omega^* = \lambda_{44} + \gamma\beta^2\omega_0/[M_0(\Omega^2 - \omega_k^2)]$. Obviously, the right side of the second equation (21) is sensitive to a change in the direction of spontaneous magnetization in domains, which ensures the possibility of refractive interaction of the wave with DW.

Now, in view of the indicated "magnetic discontinuity" at $y = y_{DW}$, the solution of the second equation (21) is not reduced to the solution for a single-domain crystal. In addition to the terms proportional to $u_z^{(j)}$, the potentials φ_j as solutions of (21) will have additional components Φ_j that are not directly related to shear waves in the domains. Therefore, representing φ_j in the form

$$\varphi_j = (-1)^{j+1}\frac{4\pi\gamma\beta\omega_0}{\Omega^2 - \omega_k^2}u_j + \Phi_j\,, \tag{22}$$

it can be seen on the basis of the second of Eqs. (21) that Φ_j is a solution to the Laplace equation

$$\nabla^2\Phi_j = 0\,. \tag{23}$$

The formation of magnetostatic fields corresponding to the potentials Φ_j can be explained by the fact that magnetic poles will be induced on the domain wall as a "magnetic discontinuity" under the action of the incident shear wave. The poles oscillate in time and are distributed along DW in agreement with the spatial periodicity of the shear displacement field on the wall. The potentials Φ_j will thus represent the stray fields of the indicated magnetic poles on both sides of the wall (see Fig. 1(b)). The localization of the sources of the scattering fields on the wall and the requirement that the solution of the Laplace equation (23) be bounded in the entire considered space show that the scattering fields should weaken with distance from the wall, roughly within $1/k_x$.

The first of Eq. (21) admits a solution in the form of plane harmonic waves with the dispersion

$$k^2 = k^2(\Omega) = \frac{\rho\Omega^2}{\lambda_\Omega^*} \tag{24}$$

Following the usual algorithm for solving refraction problems, we establish the frequency ω and the wave vector of the incident wave $k = \mathbf{n}k$, where $\mathbf{n} = (\sin\theta, -\cos\theta)$, $k = k(\omega)$ is the wavenumber determined from (24), where Ω is replaced by ω. The wave refracted on the moving DW is characterized by the frequency ω' and the wave vector $k' = \mathbf{n}'k'$ with the wave direction defined by $\mathbf{n}' = (\sin\theta', \cos\theta')$ and the wave number $k' = k(\omega')$, which is obtained by Eq. (21) by replacing Ω with ω'.

The connection between the frequencies ω, ω' and the angles θ, θ' is established from the requirement of phase conjugation of wave fields on DW. From the equality of the projections of the wave vectors of the incident and refracted waves at $y = y_{DW}$ we obtain

$$\frac{\omega}{v}\sin\theta = \frac{\omega'}{v'}\sin\theta' \equiv k_T\,, \tag{25}$$

while the time synchronization of the oscillation phases on the DW is provided by the relations

$$\omega\left(1 + \frac{V_{DW}}{v}\cos\theta\right) = \omega'\left(1 - \frac{V_{DW}}{v'}cos\theta'\right) \equiv \tilde{\omega} \tag{26}$$

In Eqs. (25) and (26) $v = \omega/k$ and $v' = \omega'/k'$ are the phase velocities of the incident and refracted waves, respectively. Taking into account Eq. (24), one can show the equivalence of Eqs. (25) and (26) to

$$\begin{aligned} &\sin\theta' + \frac{V_D}{v}\sin(\theta + \theta') \\ &= \frac{\sin\theta}{v}c_t\left[1 + \frac{\chi\omega_0^2}{\omega^2 f^2(\theta,\theta') - \omega_k^2}\right]^{1/2} \end{aligned} \tag{27}$$

$$\frac{\omega'}{\omega} = 1 + \frac{V_D}{v}\frac{\sin(\theta + \theta')}{\sin\theta'} \equiv f(\theta,\theta') \tag{28}$$

where $\chi = \gamma\beta^2/(\omega_0\lambda_{44}M_o)$ is the dimensionless constant of magnetoelastic interaction, c_t is the speed of transverse sound.

Since θ, ω and, therefore $v = v(\omega)$, are known, Eq. (27) defines θ' as the solution of this transcendental equation. The corresponding value of ω' is calculated by Eq. (28), that indicates the presence of a Doppler shift in the refracted wave. The first of the two solutions to Eq. (27) $\theta' = \pi - \theta$ exists only for large refraction angles $\theta' > \pi/2$, and does not depend on V_{DW}. Thus, a refracted wave is described by a set of values ω, v, k, that are identical to the corresponding values of the incident wave. Moreover, it is obvious that under conditions when the refraction problem makes sense, this wave should be associated with the propagation region $y < y_{DW}$. As a result, the solution $\theta' = \pi - \theta$ of Eq. (27) will correspond to the directly transmitted shear wave.

The second solution of Eq. (27) (for $\theta' \neq \pi - \theta$) can be obtained numerically. The resulting dependencies $\theta'(\theta)$ are shown in Fig. 3 for a

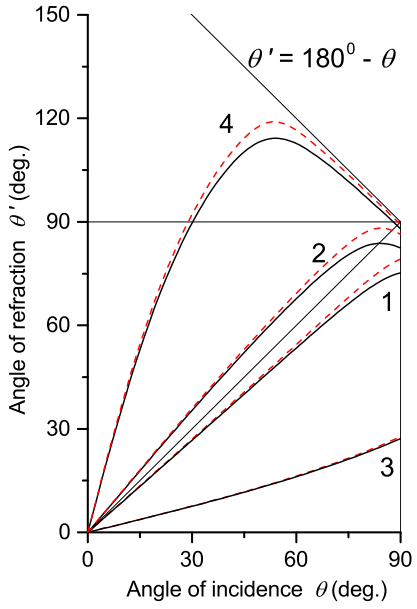

Fig. 2. Dependence of θ' on θ. Black solid curves are for $\omega = 1.005 \cdot \omega_k$, red dashed curves are for $\omega = 1.01 \cdot \omega_0$, curves marked by '1' are for $V_{DW}/c_t = 0.05$, curves marked by '2' are for $V_D/c_t = -0.1$, curves marked by '3' are for $V_D/c_t = 0.6$, curves marked by '4' are for $V_{DW}/c_t = -0.6$.

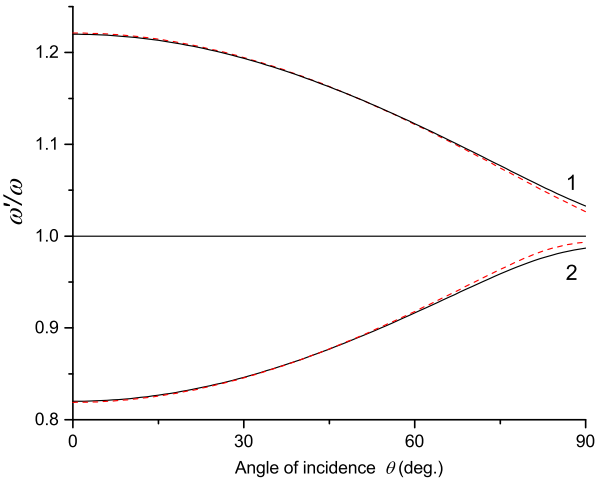

Fig. 3. Dependence of ω'/ω on θ. Black solid curves are for $\omega = 1.005 \cdot \omega_k$, red dashed curves are for $\omega = 1.01 \cdot \omega_0$, curves marked by '1' are for $V_{DW}/c_t = 0.1$, curves marked by '2' are for $V_{DW}/c_t = -0.1$.

number of values V_{DW}/c_t in the vicinity of the frequency ω_0 as well as frequencies $\omega > \omega_k$, respectively, by dashed and solid curves. Positive values of $V_{DW}/c_t > 0$ correspond to the case of reflection of a shear wave from an approaching domain wall (curves 1, 3), while at $V_D/c_t < 0$ (curves 2, 4), the incident wave interacts with the receding domain wall. The difference between the curves corresponding to different frequencies at $\theta' \to \pi - \theta$ (line $\theta' = \pi - \theta$ in Fig. 3 corresponds to the law of refraction $\theta' = \pi - \theta$ for a directly transmitted wave) is explained by the significant frequency dispersion of the refracted wave due to the Doppler approximation shown in Eqs. (27) and (28) ω' to ω_k in the case of solid curves. In the vicinity of the FMR, the frequencies of the incident wave, and even more so of the waves reflected at $V_D/c_t < 0$, are in the region where the frequency dispersion is practically absent, $v(\omega) = v(\omega') \approx c_t$. Then, as the curve '2' in Fig. 3 gives $\omega' < \omega$, from Eq. (27) we always have $\theta' > \theta$, which means the absence of the indicated bend. The change in the refractive characteristics of the reflected shear wave due to the motion of the DW is qualitatively similar to the previously known results obtained for problems with moving boundaries such as a traveling parameter wave under conditions of a complex aberration effect [46].

Fig. 3 shows typical dependencies of ω'/ω on θ. The presented behavior indicates that the shear wave is reflected from the approaching DW at a smaller angle θ' than the angle of incidence θ (curves 1, 3 in Fig. 3 lie below the $\theta = \theta'$ line) and, at the same time, show an increase of frequency due to the Doppler effect: $\omega' > \omega$ (curves 1 in Fig. 3). The opposite takes place if the wave is reflected by the retreating DW (see curves 2, 4 in Fig. 3, curve 2 in Fig. 3): $\theta' > \theta$, $\omega' < \omega$.

5. Calculation of reflection coefficients

In the case of DW motion under the action of a shear wave, the domain wall will move away with respect to the incident wave, i.e. $V_{DW} < 0$. We restrict ourselves to the case of reflection. That is, we restrict the amplitudes of the shear displacement so that the obtained DW velocities are such that the case of large refraction angles (see Fig. 2) cannot be realized. As further calculation shows, this is the case for the shear displacement amplitudes $u_z < 10^{-9}$ cm, at which the linear approximation that we use holds (small dynamic additions **h**, **m**).

In the absence of a direct connection, there are, however, boundary conditions linking the scattering fields of Eq. (23)) with acoustic waves in the domains. Acoustic boundary conditions are expressed here by the continuity of $u_z^{(j)}$ and of the shear stress tensor component $\mathbf{T}_{yz}^{(j)}$ orthogonal to the wall:

$$u_z^{(1)}\Big|_{y=y_D} = u_z^{(2)}\Big|_{y=y_D}, \quad T_{yz}^{(1)}\Big|_{y=y_D} = T_{yz}^{(2)}\Big|_{y=y_D}. \tag{29}$$

In addition, it is necessary to add electrodynamic boundary conditions [39] for the continuity of the normal components of the magnetic induction vectors $b_y^{(j)} = 4\pi m_y^{(j)} + h_y^{(j)}$ and the tangential components of the magnetic field strengths $h_x^{(j)}$ on the wall. The latter is equivalent to the requirement for the continuity of the magnetic potential. Thus, we also have

$$\left[4\pi m_y^{(1)} - \frac{\partial \varphi_1}{\partial y}\right]\Bigg|_{y=y_D} = \left[4\pi m_y^{(2)} - \frac{\partial \varphi_2}{\partial y}\right]\Bigg|_{y=y_D}, \qquad \varphi_1\big|_{y=y_D} = \varphi_2\big|_{y=y_D}. \tag{30}$$

Based on Eqs. (21), where $M_0 \to (-1)^{j+1} M_0$, $H_i \to (-1)^{j+1} H_i$ and also taking into account Eqs. (13) and (21), it can be shown that in the case of harmonic waves the quantities $m^{(j)y}$ entering in Eq. (30), and expressions for the quantities $T_{yz}^{(j)}$ can be written as

$$\begin{aligned} T_{yz} &= T_{zy} = \lambda_{44}\frac{\partial u_z}{\partial y} + 2b_{44} M_o m_y \\ m_y^{(j)} &= \frac{\gamma\beta}{\Omega^2 - \omega_k^2}\left[i\Omega\frac{\partial u_z^{(j)}}{\partial x} + (-1)^{j+1}\omega_0\frac{\partial u_z^{(j)}}{\partial y}\right] \\ &\quad + \frac{\omega_m}{4\pi(\Omega^2 - \omega_0^2)}\left[\omega_0\frac{\partial \Phi_j}{\partial y} + (-1)^{j+1} i\Omega\frac{\partial \Phi_j}{\partial x}\right] \end{aligned} \tag{31}$$

$$\begin{aligned} T_{yz}^{(j)} &= \lambda_\Omega^* \frac{\partial u_z^{(j)}}{\partial y} + (-1)^{j+1} i\Omega \frac{\gamma\beta^2}{M_o(\Omega^2 - \omega_k^2)}\frac{\partial u_z^{(j)}}{\partial x} \\ &\quad + \frac{\gamma\beta}{4\pi(\Omega^2 - \omega_0^2)}\left[i\Omega\frac{\partial \Phi_j}{\partial x} + (-1)^{j+1}\omega_0\frac{\partial \Phi_j}{\partial y}\right] \end{aligned} \tag{32}$$

The solution of the first of Eqs. (21) and all of the above can be represented in the form

$$\begin{aligned} &u_z^{(1)} = \\ &U\exp(ik_x x)[\exp(-ik_y y - i\omega t) + R\exp(ik_y' y - i\omega' t)], \\ &y > y_D \quad \text{and} \\ &u_z^{(2)} = \\ &UT\exp(ik_x x - i\omega t)\exp(-ik_y y), \quad y < y_D \end{aligned} \tag{33}$$

In order to satisfy the boundary (at $y = y_{DW}$) conditions (29), (30), the quantities Φ_j should be represented as a phase exponent, restricted by coordinate- and time invariants, i.e. $\Phi_j \sim \exp[ik_x x - i(\omega + kV_{DW}\cos\theta)t]$. Therefore, from Eq. (23) we obtain $\Phi_j \sim f_j \exp(\pm k_j y)$, where $f_j(t)$ is an arbitrary normalizing function of time, chosen for reasons of boundary condition for Φ_j in the form: $f_j = \exp(\pm y_{DW} k_x)$, $y_{DW} = V_{DW} t$.

As a result, we obtain

$$\begin{aligned}\Phi_1 &= C\exp[ik_x x - i(\omega + kV_{DW}\cos\theta)t]\exp(-k_x(y - y_{DW})),\\ &(y > y_D), \quad \text{and}\\ \Phi_2 &= D\exp[ik_x x - i(\omega + kV_{DW}\cos\theta)t]\exp(k_x(y - y_{DW})),\\ &(y < y_D).\end{aligned} \tag{34}$$

Substituting $u_z^{(j)}$ from (33) and Φ_j from (34) into boundary conditions (29), (30), and taking into account Eqs. (31), (32), (27), and (28), we obtain a system of algebraic equations for unknowns C, D, R, T. The solution of those gives us:

$$\begin{aligned}R &= -\frac{i\frac{\gamma\beta^2}{\lambda^*_\omega M_0}\Gamma_+(\omega',\omega)\tan\theta}{\left(1 + \frac{\lambda^*_{\omega'}}{\lambda^*_\omega}\tan\theta\cot\theta'\right) + i\frac{\gamma\beta^2}{\lambda^*_\omega M_0}\Gamma_+(\omega',\omega)\tan\theta},\\ T &= \frac{\left(1 + \frac{\lambda^*_{\omega'}}{\lambda^*_\omega}\tan\theta\cot\theta'\right) + i\frac{\gamma\beta^2}{\lambda^*_\omega M_0}\Gamma_-(\omega',\omega)\tan\theta}{\left(1 + \frac{\lambda^*_{\omega'}}{\lambda^*_\omega}\tan\theta\cot\theta'\right) + i\frac{\gamma\beta^2}{\lambda^*_\omega M_0}\Gamma_+(\omega',\omega)\tan\theta}\end{aligned} \tag{35}$$

where

$$\begin{aligned}\Gamma_\pm(\Omega,\omega) &= \frac{\Omega - \omega_m F(\Omega)}{\Omega^2 - \omega_k^2} \pm \frac{\omega - \omega_m F(\mp\omega)}{\omega^2 - \omega_k^2},\\ F(\Omega) &= \frac{\Omega(\omega' - \omega) + \omega_0(\omega' + \omega) - 2\omega_k^2}{2\omega'\omega - (2\omega_0 + \omega_m)(\omega' + \omega) + 2\omega_k^2}\end{aligned} \tag{36}$$

Eqs. (35), (36) represent the general solution of the boundary conditions problem of reflection of a shear wave from a uniformly moving DW [47]. For $V_D \to 0$ ($\omega' \to \omega, \theta' \to \theta, \lambda^*_{\omega'} \to \lambda^*_\omega$) Eq. (35) gives the solution for the static case:

$$R = -\frac{i\frac{\gamma\beta^2}{\lambda^*_\omega M_0}(\omega^2 - \omega_k^2)^{-1}[\omega - \omega_0\omega_m/(\omega - \omega_0)]\tan\theta}{1 + i\frac{\gamma\beta^2}{\lambda^*_\omega M_0}(\omega^2 - \omega_k^2)^{-1}[\omega - \omega_0\omega_m/(\omega - \omega_0)]\tan\theta} \tag{37}$$

It follows from expressions (35), (37) that at normal incidence $\theta = 0$ the reflection coefficient is zero due to the absence of magnetic poles on the domain wall as a "magnetic discontinuity". Such poles can be formed by the magnetostrictive mechanism only in the case of an oblique incidence of a shear wave. Therefore, in Ref. [37], a bias field was required for the DW motion at normal incidence of the wave. This field turns out to be fundamentally necessary for the dispersion laws of magnetoelastic waves to the right and left of the DW to differ and for the DW itself to create an inhomogeneity for the wave. Otherwise, at $R = 0$ there will be no motion of the domain wall under the action of ultrasound. The more detailed discussion and calculation of amplitudes C and D is given in Appendix.

6. Numerical modeling

If we look closely at the system of nonlinear equations formed by Eqs. (19), (27), (28) and (35), we can see that we have three unknowns V_D, R, θ', that can be calculated as a function of the amplitude u_z and the angle of incidence θ. Let us first define the frequency range that will be interesting for the calculation. As can be seen from Eq. (37), in the absence of motion, the reflection coefficient reaches unity for the FMR frequency $\omega = \omega_0$. At this frequency, resonant excitation of magnetostatic potential fields Φ_j (see Eq. (23)) occurs resulting in a resonant reflection of the wave. The motion of DW affects the resonant frequency established by the poles of the functions $F(\omega)$, $F(\omega')$ (36) in the vicinity of the lower boundary of the Walker frequency spectrum in accordance with (27), (28) and the equation

$$\omega'_F = \omega' = \omega_0 + \omega_m(\omega - \omega_0)[2(\omega - \omega_0) - \omega_m]^{-1} \tag{38}$$

Since the reflection of the shear wave occurs from the DW moving in the same direction as the wave propagation, we should consider frequencies somewhat higher than the FMR frequency.

The numerical solution of Eqs. (19), (27), (28), (35) is shown in Figs. 4 and 5. The material parameters that were used in these calculations are taken for yttrium iron garnet (YIG) from literature [38,40,41] and are summarized in Table 1. The choice of the YIG as an ideal material to be used in our numerical calculations is due to the fact that it possesses an exceptionally low damping in both magnetic and elastic systems. Because of this, YIG is widely used in experiments both in the field of domain wall motion and propagation of magnetoelastic waves [48,49] and as such represents a straightforward basis for application of our theory.

As can be seen from Fig. 4, for a small detuning of the frequency of the incident wave from the FMR, shown by solid black line, comparatively small values of the amplitude of the acoustic wave $u_z \approx 10^{-10}$ cm are required for the frequency of the reflected wave to fall on the resonant frequency determined by formula (38). Moreover, the DW velocity for this frequency detuning is approximately 0.001 of the speed of shear waves in YIG. The shape of the resonant reflection peak can be described as "classical", i.e. to the left of the maximum there is a positive slope of the curve, and to the right of it is a negative slope.

It can be seen from Fig. 4 that the larger the detuning from the FMR frequency, the larger the values of the shear wave amplitude are

Table 1
YIG crystal parameters.

Parameter name	Value
Gyromagnetic ratio	$\gamma = 2 \cdot 10^7$
Shear modulus	$\lambda_{44} = 7.64 \cdot 10^{11}$
Shear wave speed	$c_t = 3.8 \cdot 10^5$ cm/s
Magnetization	$M_0 = 140$ G
Internal field	$H_i = 700$ Oe
Magnetoelastic interaction constant	$\beta = 7.4 \cdot 10^6$ erg/cm^3
Ferromagnetic resonance frequency	$\omega_0 = \gamma H_i = 1.4 \cdot 10^{10}$ rad/s^{-1} ($\nu_0 = 2.23$ GHz)
Magnetoelastic resonance frequency	$\omega_k \approx 2.619 \cdot 10^{10}$ rad/s^{-1} ($\nu_k = 4.17$ GHz)
$\gamma\beta^2/\lambda_{44}M_0$	$\approx 1.023 \cdot 10^7$ rad/s^{-1}
Magnetostatic frequency	$\omega_m = 4\pi\gamma M_0 \approx 3.5 \cdot 10^{10}$ rad/s^{-1}
YIG crystal density	$\rho = 5.2$ g/cm^3

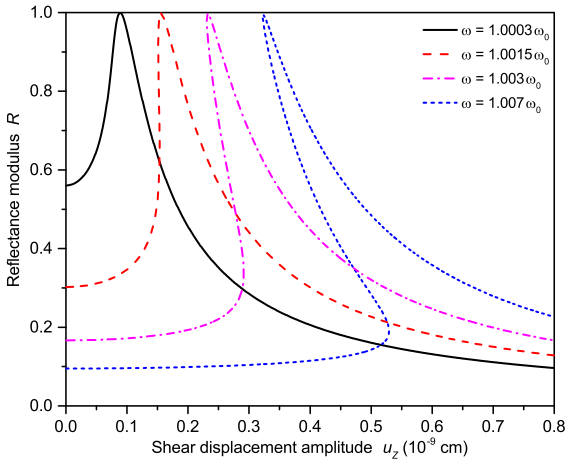

Fig. 4. Modulus of the reflection coefficient as a function of the amplitude of the shear displacement for the vicinity of the FMR frequency $\omega_0 = 1.4 \cdot 10^{10}$ rad/s ($\nu_0 = 2.23$ GHz). Here and in the next figure we show frequencies as $\omega = 1.0003\omega_0$, $1.0015\omega_0$, $1.003\omega_0$, $1.007\omega_0$.

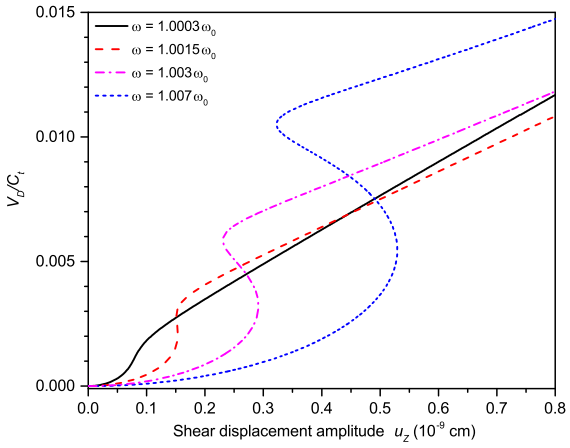

Fig. 5. Dependence of the ratio of DW velocity to the speed of sound on the shear displacement amplitude (cm) for the vicinity of the FMR frequency $\omega_0 = 1.4 \cdot 10^{10}$ rad/s ($\nu_0 = 2.23$ GHz).

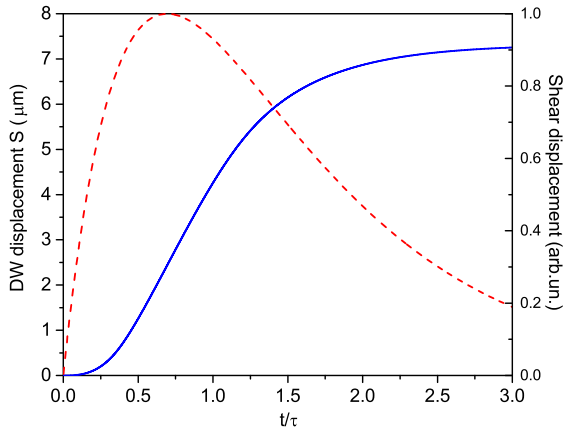

Fig. 6. Time dependence of the DW displacement, calculated for $\tau = 10^{-6}$ s and $u_{z0} = 10^{-9}$ cm.

required to achieve resonance, at which the modulus of the reflection coefficient reaches unity. In the resonance region, the DW velocity reaches velocities of the order of several percent of the shear wave velocity in YIG. In this case, a slope of the peak appears in the form of a resonance curve in the direction of a decrease in the amplitude of shear waves. This bistable form of the resonance curve is typical for nonlinear oscillatory systems (see [32]). Magnetoelastic bistability observed in many magnetic systems (e.g. hematite [33]) at a high power level was investigated both theoretically and experimentally. The bistability is induced by the strong coupling between the acoustic and magnetic subsystems. In our case, the manifestation of nonlinearity only occurs for sufficiently large amplitudes $u_z > 2 \cdot 10^{-10}$ cm.

In experiments, it is customary to measure the DW displacement as a function of time, since the control signal has, as a rule, the shape of a pulse. Fig. 6 shows the magnitude of the displacement of the DW as a function of time. We set the shape of the time dependence of the displacement amplitude in the simplest form

$$u_z = u_{z0}(1 - \exp(-t/\tau))\exp(-t/\tau) \cdot \exp[-i\omega t], \quad (39)$$

where τ sets the "duration" of the control signal.

It can be seen that for a pulse duration $\tau = 10^{-6}$ s, the DW moves for several micrometers and thus shows average velocity of several meters per second, which is quite enough to observe it experimentally.

In fact, some experiments in a similar direction have been carried out, see for example [50], where short laser pulses were used. However, for a reliable and quantitative confirmation of our theory, first, one needs shear acoustic waves. Laser-induced excitation of these in low-symmetry crystals and their influence on magnetization has been recently demonstrated in [51,52]. The microsecond timescale pulses that lead to sizeable effects, can be obtained by using a microsecond-long bunch of single pulses in succession, e.g. from 80–100 MHz Ti:sapphire laser, and having in mind long lifetime of the elastic excitations. However, such excitation produces very broadband wave packets. Therefore, alternatively, one could use longer pulses of acoustic waves at specific frequency resonantly generated by interdigital transducers [53,54]. Particularly using this last approach, the effects of propagating shear acoustic waves on DW should be directly observable, including its characteristic dependence of the frequency of elastic waves and the appearing nonlinear effects.

7. Conclusion

To summarize, here we have theoretically shown the possibility of triggering the motion of a magnetic domain wall by means of an acoustic shear wave incident at an angle onto the plane of DW. In this case, the motion of the DW can be induced without the need of an extra bias magnetic field. It is shown that at sufficiently large amplitudes of the shear displacement, the speed of the forced motion can reach several percent of the speed of sound. This is fully sufficient to be able to observe this displacement in the experiment. It was found that at certain angles of incidence and shear displacement amplitudes, resonant reflection of the acoustic wave occurs and nonlinearity may appear due to the interaction of the elastic and magnetic subsystems. Nonlinearity is expressed by a negative slope of the resonance reflection peak and an s-shaped dependence in the resonance region of the domain wall velocity on the shear displacement amplitude, which is typical for nonlinear systems. The described approach can in principle be applied to the description of both weak ferromagnets and antiferromagnets. For this, however, a system of coupled Landau–Lifshitz equations need to be solved, which will be a subject of a separate detailed study. Within the framework of the described model, we do not consider the interaction of a moving domain wall with an acoustic wave (see for more details [55,56]). The established behavior of the induced DW motion can be used to implement the elements of integral spintronics (logic circuits, memory elements, etc.), as well as to increase the efficiency of information technologies.

Declaration of competing interest

The authors declare that they have no known competing financial interests or personal relationships that could have appeared to influence the work reported in this paper.

Acknowledgments

This study was supported in part by the Russian Foundation for Basic Research (projects numbers 18-29-27020, 19-29-03015, 18-52-16006) and by the grant from the Government of the Russian Federation for state support of scientific research conducted under the guidance of leading scientists in Russian higher education institutions, research institutions, and state research centers of the Russian Federation (project number 075-15-2019-1874). A part of the study was carried out within a state assignment for the Kotelnikov Institute of Radio Engineering and Electronics, Russian Academy of Sciences. P.A. acknowledges the support from the RFBR (project number 19-32-90242). We gratefully acknowledge the Nederlandse Organisatie voor Wetenschappelijk Onderzoek (NWO-I), Netherlands for their financial contribution, including the support of the FELIX Laboratory. We also acknowledge support from the COST Action CA17123 "Ultrafast opto-magneto-electronics for non-dissipative information technology" (MAGNETOFON).

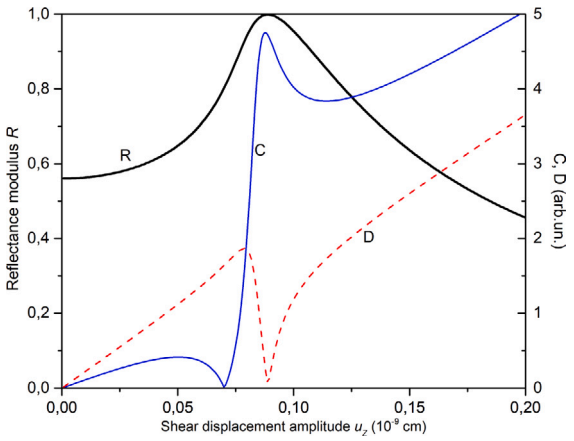

Fig. 7. The dependence of the reflection coefficient (black curve), the amplitudes C (blue curve) and D (red curve) as a function of the amplitude of the shear displacement, where $\omega = 1.0003 \cdot \omega_0$.

Appendix

Substituting $u_z^{(j)}$ from (33) and Φ_j from (34) into the boundary conditions (29), (30), and taking into account expressions (27), (28), (31), and (32), we obtain a system of algebraic equations for unknown variables C, D, R, T:

$$1 + R = T, \tag{40}$$

$$\begin{aligned}\lambda_\omega^* U \cdot (-ik_y) + \lambda_\omega^* R \cdot U \cdot ik_y' - k_x\left(\frac{\omega U\gamma \cdot \beta^2}{M_0(\omega^2 - \omega_k^2)} + \frac{\omega'\gamma \cdot \beta^2 R}{M_0(\omega'^2 - \omega_k^2)}\right)\\ -\frac{k_x \cdot \gamma \cdot \beta}{(\omega - \omega_0)}C - \frac{k_x \cdot \gamma \cdot \beta}{(\omega' - \omega_0)}C = \lambda_\omega^* \cdot U \cdot T(-ik_y)\\ +k_x\omega \cdot U \cdot T\frac{\gamma\beta^2}{M_0(\omega^2 - \omega_k^2)} - \frac{k_x \cdot \gamma \cdot \beta}{\omega - \omega_0}D,\end{aligned} \tag{41}$$

$$\begin{aligned}-\frac{4\pi\gamma\beta\omega k_x}{\omega^2 - \omega_k^2}U - \frac{4\pi\gamma\beta\omega' k_x}{\omega'^2 - \omega_k^2}UR - \frac{\omega_m k_x}{(\omega - \omega_0)}C - \frac{\omega_m k_x}{\omega' - \omega_0}C + 2Ck_x\\ = -\frac{4\pi\gamma\beta\omega k_x}{\omega^2 - \omega_k^2}UT + \frac{\omega_m k_x}{(\omega - \omega_0)}D - Dk_x,\end{aligned} \tag{42}$$

$$\frac{4\pi\gamma\beta\omega_0}{\omega^2 - \omega_k^2}U + \frac{4\pi\gamma\beta\omega_0}{\omega'^2 - \omega_k^2}UR + 2C = -\frac{4\pi\gamma\beta\omega_0}{\omega^2 - \omega_k^2}UT + D, \tag{43}$$

where U is the amplitude of u_z. The numerical solution of the described system (40)–(43) for C and D is presented in Fig. 7.

The amplitude D of the magnetic potential Φ_j from the other side of the DW (namely, $j = 2$ for $y < y_{DW}$, see explanation after Eq. (20)) is minimal. The minimum of the amplitude C respects to the resonant transmission of the magnetoelastic wave through the DW. In addition, we should note that the slope of the resonant curves C and D in the nonlinear region (the region of large u_z, Fig. 4) is similar to the slope of the magnetoelastic wave reflection coefficient (Fig. 4).

References

[1] E. Beaurepaire, J.-C. Merle, A. Daunois, J.-Y. Bigot, Ultrafast spin dynamics in ferromagnetic nickel, Phys. Rev. Lett. 76 (1996) 4250.

[2] F. Hansteen, A. Kimel, A. Kirilyuk, T. Rasing, Nonthermal ultrafast optical control of the magnetization in garnet films, Phys. Rev. B 73 (2006) 014421.

[3] M. van Kampen, C. Jozsa, J.T. Kohlhepp, P. LeClair, L. Lagae, W.J.M. de Jonge, B. Koopmans, All-optical probe of coherent spin waves, Phys. Rev. Lett. 88 (2002) 227201.

[4] T. Satoh, Y. Terui, R. Moriya, B.A. Ivanov, K. Ando, E. Saitoh, T. Shimura, K. Kuroda, Directional control of spin-wave emission by spatially shaped light, Nature Photonics 6 (10) (2012) 662–666.

[5] C. Stanciu, F. Hansteen, A. Kimel, A. Kirilyuk, A. Tsukamoto, A. Itoh, T. Rasing, All-optical magnetic recording with circularly polarized light, Phys. Rev. Lett. 99 (4) (2007) 047601.

[6] C.-H. Lambert, S. Mangin, B.S.D.C.S. Varaprasad, Y.K. Takahashi, M. Hehn, M. Cinchetti, G. Malinowski, K. Hono, Y. Fainman, M. Aeschlimann, E.E. Fullerton, All-optical control of ferromagnetic thin films and nanostructures, Science 345 (2014) 1337.

[7] A. Stupakiewicz, K. Szerenos, D. Afanasiev, A. Kirilyuk, A.V. Kimel, Ultrafast nonthermal photo-magnetic recording in a transparent medium, Nature 542 (2017) 71.

[8] A.A. Bukharaev, A.K. Zvezdin, A.P. Pyatakov, Y.K. Fetisov, Straintronics: a new trend in micro- and nanoelectronics and materials science, Phys.-Usp. 61 (2018) 1175.

[9] J.D. Caldwell, L. Lindsay, V. Giannini, I. Vurgaftman, T.L. Reinecke, S.A. Maier, O.J. Glembocki, Low-loss, infrared and terahertz nanophotonics using surface phonon polaritons, Nanophotonics 4 (2015) 44.

[10] H. Miao, F. Li, Shear horizontal wave transducers for structural health monitoring and nondestructive testing: A review, Ultrasonics 114 (2021) 106355.

[11] K. Roy, S. Bandyopadhyay, J. Atulasimha, Hybrid spintronics and straintronics: A magnetic technology for ultra low energy computing and signal processing, Appl. Phys. Lett. 99 (2011) 063108.

[12] K. Roy, Ultra-low-energy straintronics using multiferroic composites, Proc. SPIE 9167 (2014) 91670U.

[13] O. Kovalenko, T. Pezeril, V.V. Temnov, New concept for magnetization switching by ultrafast acoustic pulses, Phys. Rev. Lett. 110 (2013) 266602.

[14] D.A. Bozhko, V.I. Vasyuchka, V. Chumak, A.A. Serga, Magnon-phonon interactions in magnon spintronics, Fiz. Nizk. Temp. 46 (2020) 462.

[15] A.V. Scherbakov, A.S. Salasyuk, A.V. Akimov, X. Liu, M. Bombeck, C. Brüggemann, D.R. Yakovlev, V.F. Sapega, J.K. Furdyna, M. Bayer, Coherent magnetization precession in ferromagnetic (Ga,Mn)As induced by picosecond acoustic pulses, Phys. Rev. Lett. 105 (2010) 117204.

[16] N.I. Polzikova, S.G. Alekseev, V.A. Luzanov, A.O. Raevskiy, Acoustic excitation and electrical detection of spin waves and spin currents in hypersonic bulk waves resonator with YIG/Pt system, J. Magn. Magn. Mater. 479 (2019) 38–42.

[17] S. Giordano, Y. Dusch, N. Tiercelin, P. Pernod, V. Preobrazhensky, Elastically driven ferromagnetic resonance in nickel thin films, Phys. Rev. Lett. 106 (2011) 117601.

[18] N. Ogawa, W. Koshibae, A.J. Beekman, N. Nagaosa, M. Kubota, M. Kawasaki, Y. Tokura, Photodrive of magnetic bubbles via magnetoelastic waves, Proc. Natl. Acad. Sci. 112 (29) (2015) 8977–8981.

[19] A. Stupakiewicz, C.S. Davies, K. Szerenos, D. Afanasiev, K.S. Rabinovich, A.V. Boris, A. Caviglia, A.V. Kimel, A. Kirilyuk, Ultrafast phononic switching of magnetization, Nat. Phys. 17 (2021) 489.

[20] D.A. Allwood, G. Xiong, C. Faulkner, D. Atkinson, D. Petit, R. Cowburn, Magnetic domain-wall logic, Science 309 (5741) (2005) 1688–1692.

[21] S.S. Parkin, M. Hayashi, L. Thomas, Magnetic domain-wall racetrack memory, Science 320 (5873) (2008) 190–194.

[22] D. Xua, F. Caia, M. Chena, F. Lia, C. Wanga, L. Meng, D. Xu, W. Wang, J. Wu, H. Zheng, Acoustic manipulation of particles in a cylindrical cavity: Theoretical and experimental study on the effects of boundary conditions, Ultrasonics 93 (2019) 18.

[23] X. Penga, W. Hea, F. Xina, G.M. Genind, T.J. Lub, The acoustic radiation force of a focused ultrasound beam on a suspended eukaryotic cell, Ultrasonics 108 (2020) 106205.

[24] L. Zeng, J. Zhanga, Y. Liu, Y. Zhao, N. Hua, Asymmetric transmission of elastic shear vertical waves in solids, Ultrasonics 96 (2019) 34.

[25] H. Zhou, J. Zhanga, P. Fenga, D. Yu, Z. Wu, An amplitude prediction model for a giant magnetostrictive ultrasonic transducer, Ultrasonics 108 (2020) 106017.

[26] R. Kryshtal, A. Medved, Surface acoustic waves in dynamic magnonic crystals for microwave signals processing, Ultrasonics 94 (2019) 60.

[27] B. Bolotovskij, S. Stoljarov, Reflection of light from a moving mirror and related problems, Sov. Phys.-Usp. 32 (9) (1989) 813–827, (Translation of Uspekhi Fizicheskikh Nauk).

[28] G.I. Freidman, Otrazhenie jelektromagnitnyh voln v girotropnyh sredah ot volny magnitnogo polja, JETP Lett. 41 (1) (1961) 226–233, (Translation of Pis'ma v Zhurnal Eksperimental'noi i Teoreticheskoi Fiziki).

[29] S. Demokritov, A. Kirilyuk, N. Kreines, V. Kudinov, V. Smirnov, M. Chetkin, Inelastic light scattering by a dynamic domain wall, JETP Lett. 48 (1988) 294, (Translation of Pis'ma v Zhurnal Eksperimental'noi i Teoreticheskoi Fiziki).

[30] S. Demokritov, A. Kirilyuk, N. Kreines, V. Kudinov, V. Smirnov, M. Chetkin, Interaction of the moving domain wall with phonons, J. Magn. Magn. Mater. 102 (1991) 339.

[31] B. Auld, C. Tsai, Doppler conversion and adiabatic time domain conversion of acoustic and spin waves, Appl. Phys. Lett. 9 (5) (1966) 192–194.

[32] V.I. Ozhogin, V.L. Preobrazhenskii, Nonlinear dynamics of coupled systems near magnetic phase transitions of the "order-order" type, J. Magn. Magn. Mater. 100 (1-3) (1991) 544–571.

[33] Y.K. Fetisov, V.L. Preobrazhenskii, P. Pernod, Bistability in a nonlinear magnetoacoustic resonator, J. Commun. Technol. Electron. 51 (2) (2006) 218–230.

[34] T. Hayashi, K. Ishihara, Generation of narrowband elastic waves with a fiber laser and its application to the imaging of defects in a plate, Ultrasonics 77 (2017) 47.
[35] M. Lejman, G. Vaudel, I.C. Infante, P. Gemeiner, V.E. Gusev, B. Dkhil, P. Ruello, Giant ultrafast photo-induced shear strain in ferroelectric BiFeO 3, Nature Commun. 5 (1) (2014) 1–7.
[36] B.P. Sorokin, G.M. Kvashnin, A.S. Novoselov, V.S. Bormashov, A.V. Golovanov, S.I. Burkov, V.D. Blank, Excitation of hypersonic acoustic waves in diamond-based piezoelectric layered structure on the microwave frequencies up to 20 GHz, Ultrasonics 78 (2017) 162–165.
[37] P.E. Zil'berman, A.V. Umansky, Pressure of spin and ultrasonic-waves on the bloch domain boundary in the monoaxial ferromagnetic, Sov. Phys.—Tech. Phys. 58 (8) (1988) 1572–1576, (Translation of Zhurnal Tekhnicheskoi Fiziki).
[38] G.A. Smolensky, V.V. Lemanov, Ferrites and their Engineering Application, Nauka, 1975, (in Russian).
[39] L.D. Landau, E.M. Lifshitz, Electrodynamics of Continuous Media, Butterworth-Heinemann, 1984.
[40] Y.M. Yakovlev, S.S. Gandelev, Ferrite Monocrystals in Radio Engineering, Sov. radio, 1975, (in Russian).
[41] B.A. Goldin, L.N. Kotov, L.C. Zarembo, S.N. Karpachev, Spin-Phonon Interactions of Crystal-Ferrites, Nauka, 1991, (in Russian).
[42] A.I. Akhiezer, V.G. Bar'yakhtar, M.I. Kaganov, Spin waves in ferromagnets and antiferromagnets, Sov. Phys.-Usp. 3 (4) (1961) 567–592, (Translation of Uspekhi Fizicheskikh Nauk).
[43] L. Landau, E. Lifshits, On the theory of the dispersion of magnetic permeability in ferromagnetic bodies, Ukr. J. Phys. Spec. Issue 53 (2008) 14–22.
[44] E. Turov, A. Lugovoj, Magnetoelastic oscillations of domain walls in ferromagnets - 2. Generation and scattering of sound, Phys. Met. Metallogr. 50 (5) (1980) 1–10, (Translation of Fizika Metallov i Metallovedenie, USSR).
[45] V.S. Gornakov, L.M. Dedukh, Y.P. Kabanov, Domain wall motion in yttrium iron garnet single crystals at high temperatures, Sov. Phys.—Solid State 26 (3) (1984) 391–398.
[46] Y.M. Sorokin, Doppler effect and aberrational effects in dispersive medium, Radiophys. Quantum Electron. 36 (7) (1993) 410–422.
[47] N.S. Shevjahov, Interaction of an acoustic wave with a moving Bloch wall in an iron-garnet crystal, Akust. Zh. (Sov. Phys. Acoust.) 36 (4) (1990) 760–766.
[48] D.A. Bozhko, V.I. Vasyuchka, A.V. Chumak, A.A. Serga, Magnon-phonon interactions in magnon spintronics (Review article), Low Temp. Phys. 46 (4) (2020) 383–399.
[49] M.A. Wanas, Domain-wall motion in yttrium-iron garnets, J. Appl. Phys. 38 (3) (1967) 1019–1021.
[50] N. Ogawa, et al., Photodrive of magnetic bubbles via magnetoelastic waves, Proc. Natl. Acad. Sci. USA 112 (2015) 8977.
[51] M. Bombeck, J.V. Jäger, A.V. Scherbakov, T. Linnik, D.R. Yakovlev, X. Liu, J.K. Furdyna, A.V. Akimov, M. Bayer, Magnetization precession induced by quasitransverse picosecond strain pulses in (311) ferromagnetic (Ga, Mn)As, Phys. Rev. B 87 (6) (2013).
[52] V.N. Kats, T.L. Linnik, A.S. Salasyuk, A.W. Rushforth, M. Wang, P. Wadley, A.V. Akimov, S.A. Cavill, V. Holy, A.M. Kalashnikova, A.V. Scherbakov, Ultrafast changes of magnetic anisotropy driven by laser-generated coherent and noncoherent phonons in metallic films, Phys. Rev. B 93 (21) (2016).
[53] M. Weiler, L. Dreher, C. Heeg, H. Huebl, R. Gross, M.S. Brandt, S.T.B. Goennenwein, Elastically driven ferromagnetic resonance in nickel thin films, Phys. Rev. Lett. 106 (11) (2011).
[54] S. Datta, Surface Acoustic Wave Devices, Prentice Hall, Englewood Cliffs, 1986, 1986.
[55] K.H. Prabhakara, T.B. Shapaeva, M.D. Davydova, K.A. Zvezdin, A.K. Zvezdin, C.S. Davies, A. Kirilyuk, T. Rasing, A.V. Kimel, Controlling magnetic domain wall velocity by femtosecond laser pulses, J. Phys.: Condens. Matter 33 (7) (2020) 075802.
[56] A.S. Abyzov, B.A. Ivanov, Dynamic damping of a domain wall in a ferromagnet, Sov. Phys.—JETP 49 (5) (2020) 865–871.